J Therm Anal Calorim (2016) 126:995–1005
DOI 10.1007/s10973-016-5536-1

A study of coal chars combustion in O_2/H_2O mixtures by thermogravimetric analysis

Liang Zhang[1] · Chun Zou[1] · Di Wu[1] · Yang Liu[1] · Chuguang Zheng[1]

Received: 22 November 2015 / Accepted: 12 May 2016 / Published online: 24 May 2016

Abstract Oxy-steam combustion is a new oxy-fuel combustion technology which involves fuels burn in pure oxygen, and the high temperature is moderated using either water or steam. In this study, FG and XS char samples were prepared in a horizontal tube furnace at 1073 K under argon atmosphere. The combustion characteristics and kinetic parameters of FG and XS char in O_2/H_2O atmosphere were studied using non-isothermal thermogravimetric analysis. The results indicated that replacing N_2 by H_2O caused the improved in the combustion reactivity and performance of FG and XS char with the identical oxygen concentration. The ignition temperature, peak temperature and burnout temperature in O_2/H_2O atmosphere were lower than those in O_2/N_2 atmosphere with the identical oxygen concentration. The activation energy values of FG and XS determined by three mode-free methods decreased with the increasing conversion level, and the activation energy of FG char was less than that of XS char at the same conversion. The kinetic mechanism function calculated result based on the combination of the Popescu method and the Coats–Redfern integral method showed the combustion of FG char in O_2/H_2O atmosphere followed the first-order chemical reaction kinetic.

Keywords Oxy-steam combustion · Thermogravimetric analysis · Combustion characteristics · Kinetic analysis

✉ Chun Zou
zouchun@hust.edu.cn

[1] State Key Laboratory of Coal Combustion, Huazhong University of Science and Technology, Wuhan 430074, People's Republic of China

Introduction

Global warming caused by the presence of greenhouse gases in the atmosphere is a worldwide issue. Carbon dioxide (CO_2) is the primary greenhouse gas emitted from the combustion of fossil fuels [1]. CO_2 capture and storage (CCS) is widely recognized as a feasible method to control CO_2 emissions, and there are three main CO_2 capture approaches: post-combustion, pre-combustion and oxy-fuel combustion. Oxy-fuel combustion is considered as a promising technology for CO_2 capture, because it can feasibly produce a high CO_2 concentration in the exhaust gas (greater than 90 % by volume) that is almost sequestration-ready and has a low technical risk [2]. So, oxy-fuel combustion has attracted considerable attention in recent years [3, 4].

In 2007, the Canadian Centre for Mineral and Energy Technology (CANMET) proposed a new oxy-fuel system, namely oxy-steam combustion [5]. In this combustion mode, fuels burn in pure oxygen, and the high temperature is moderated by either water or steam. CANMET has recently developed a novel oxy-steam burner for zero emission power plants. The computational fluid dynamics (CFD) simulation and pilot-scale experimental results indicated that oxy-steam combustion led to high CO_2 concentrations (~90 %), low CO, moderate NO_x and typical SO_x levels [6]. Seepana and Jayanti proposed a power generating system based on oxy-steam combustion called steam-moderated oxy-fuel combustion (SMOC) [7]. Those authors suggested that oxy-steam combustion had many advantages over O_2/CO_2 recycle combustion, such as a compact system, easy operation, small geometry size and energy savings.

Many studies have focused on the O_2/CO_2 combustion process, and the results indicated the physicochemical

properties of dilute gas had a great influence on the combustion characteristics of coal/char [8, 9]. The physical properties of H_2O are different from N_2 and CO_2, and the chemical properties of H_2O are more active, so the combustion characteristics of coal/char under an oxy-steam atmosphere are expected to be different from conventional air combustion and O_2/CO_2 combustion.

Because of the special properties of H_2O, the studies of the effect of H_2O on the combustion process have received more and more attention. Many published works found adding H_2O had certain effects on the burning velocity and flame temperature during the combustion process of gaseous fuels [10–15]. Besides, the oxy-coal combustion process was also changed when substituting part CO_2 with H_2O [16–19].

Although some works have focused on the effect of adding steam on the combustion characteristics of gaseous fuels in different atmospheres, the combustion characteristics of coal/char in O_2/H_2O atmosphere have rarely been studied. Recently, we have carried out related studies about coal combustion in O_2/H_2O atmosphere. Thermogravimetric analysis (TG) results found the coal burning process in O_2/H_2O mixtures was delayed compared with that in O_2/N_2 mixtures [20]. The research on the ignition behaviors of pulverized coal particles in O_2/N_2 and O_2/H_2O mixtures in a drop tube furnace using flame monitoring techniques indicated the ignition of pulverized coal particles in O_2/H_2O mixtures was earlier than that in O_2/N_2 mixtures at same oxygen concentration, and the numerical simulation showed the ignition mechanism of coal particles in O_2/H_2O atmosphere was homogeneous [21, 22].

Char combustion is a most important process during coal combustion, and the study of combustion characteristics of coal chars under O_2/H_2O environment is essential to the development of large-scale test platforms. Thermogravimetric analysis is a simple and practicable approach, and it has been widely used to investigate the pyrolysis, combustion and kinetic characteristics of various fuels [23–27].

The aim of the present work is to study the oxy-steam combustion characteristics and kinetic behaviors of two coal chars obtained in argon atmosphere. In this study, the non-isothermal thermogravimetric analysis method was used to investigate the combustion characteristics of char. The activation energy values of the char samples were calculated using three model-free methods, Flynn–Wall–Ozawa (FWO), Starink and Kissinger–Akahira–Sunose (KAS), and the combustion mechanism function was ascertained by the combination of the Popescu method and the Coats–Redfern integral method.

Experimental

Char preparation

Two parent coals of a bituminous coal (FG) and a meager coal (XS) were used to prepare the char samples. The parent coals were crushed, ground with a ball mill and sieved to a particle size fraction of 45–75 μm. The char samples were prepared in a horizontal tube furnace at 1073 K in an argon atmosphere. The char samples were produced by the procedures as follows: Firstly, approximately 1 g of each coal sample was placed on a ceramic boat, and the ceramic boat was placed into the heating zone of the tube furnace. Then, the reactor was heated at a constant rate from room temperature to 1073 K, and the coal sample was kept in the reactor for 30 min at 1073 K under argon atmosphere. The argon was provided from a gas cylinder. Finally, heating was stopped, and the char sample was cooled to room temperature under argon atmosphere. The proximate and ultimate analyses of parent coals and char samples are presented in Table 1.

Oxy-steam combustion tests of coal chars

The char combustion tests were performed in a Netzsch STA449F3 thermobalance with a water vapor generator. The water control precision of the steam generator was 0.02 g h^{-1}. Approximately 5 mg of char sample was used for each experiment. The char samples were heated from room temperature to 1273 K in the mixtures of O_2/H_2O or O_2/N_2 with various oxygen concentrations (21, 30 and

Table 1 Proximate analysis and ultimate analysis of the coal and char samples

	FG coal	XS coal	FG char	XS char
Proximate analysis[a]/mass%				
Moisture	4.25	3.06	0.57	0.36
Volatile matter	32.80	18.85	2.71	1.88
Ash	4.42	12.75	10.67	18.38
Fixed carbon	58.53	65.34	78.45	79.73
Ultimate analysis[a]/mass%				
C	74.15	72.03	81.55	75.23
H	5.46	3.42	1.44	0.84
O[b]	10.33	5.37	4.52	2.21
N	1.12	1.06	1.04	0.95
S	0.27	2.31	0.21	2.03

[a] Air-dried basis

[b] By difference

40 %) at a heating rate of 20 K min^{-1}. In order to investigate the oxy-steam combustion kinetic, the non-isothermal thermogravimetric experiments were also conducted at different heating rates (10, 15, 20 and 25 K min^{-1}) in 21 % O_2/79 % H_2O mixtures. The total gas flow rate was 100 mL min^{-1}.

Determination of combustion characteristic parameters

The combustion characteristic parameters can be determined from the combustion profile, including ignition temperature (T_i), peak temperature (T_{max}), burnout temperature (T_h), maximum rate of mass loss $(dW/dt)_{max}$ and average of mass loss $(dW/dt)_{mean}$. T_i is determined by using TG–DTG extrapolation method, and the T_h is defined as the temperature at which the rate of mass loss diminishes to 1 mass% min^{-1}. T_{max} is the temperature which maximum rate of mass loss occurs. The coal reactivity index R is used to evaluate the combustion performance of char sample, defined as [23]:

$$R = \frac{1}{W_0}\frac{dW}{dt} \tag{1}$$

where W_0 is the initial dry mass of the char sample and dW/dt is the mass lose rate of char due to combustion. The greater its value, higher the combustion reactivity.

The combustion characteristic is also evaluated by a comprehensive combustion index S, which is defined as follows [24]:

$$S = \frac{(dW/dt)_{max}(dW/dt)_{mean}}{T_i^2 T_h} \tag{2}$$

The higher the S, the better the combustion performance of the char.

Kinetic analysis method

The procedure to determine the kinetic parameters is summarized as:

1. The activation energy is obtained through the FWO, Starink and KAS methods;
2. The most suitable kinetic mechanism function $G(\alpha)$ is deduced based on the Popescu method;
3. According to the most suitable kinetic mechanism function $G(\alpha)$, the activation energy E is determined by Coats–Redfern integral method;
4. By comparing the activation energies obtained through the Coats–Redfern integral method with those obtained through the FWO, Starink and KAS methods, the combustion kinetic mechanism function is determined.

Determination of the activation energy

For non-isothermal thermogravimetric experiments with constant heating rate, the reaction rate can be expressed as:

$$\frac{d\alpha}{dT} = \frac{A}{\beta}\exp\left(-\frac{E}{RT}\right)f(\alpha) \tag{3}$$

where α is the degree of conversion, $\alpha = (W_0 - W_t)/(W_0 - W_\infty)$ (W_0 and W_∞ are the mass at the beginning and at the end of reaction, respectively, and W_t is the mass at temperature T). β is the heating rate, A is the pre-exponential factor, E is the activation energy, R is the universal gas constant and $f(\alpha)$ represents the reaction mechanism function. The integration of Eq. (3) yields:

$$G(\alpha) = \int_0^\alpha \frac{d\alpha}{f(\alpha)} = \frac{A}{\beta}\int_0^T \exp\left(-\frac{E}{RT}\right)dT = \frac{AE}{\beta R}P(u) \tag{4}$$

where $u = E/(RT)$ and $P(u)$ is the temperature integral:

$$P(u) = \int_u^\infty \frac{\exp(-u)}{u^2}du \tag{5}$$

Actually, the model-free methods differ depending on the approximation of temperature integral $P(u)$.

Flynn–Wall–Ozawa (FWO) method

FWO equation relies on Doyle's approximation which gives [28–30]:

$$P(u) \cong \exp(-1.0518u - 5.3308) \tag{6}$$

This approximation leads to

$$\ln\beta = -1.0518\frac{E}{RT} + C_1 \tag{7}$$

Thus, for a constant conversion ratio α, $\ln\beta$ versus $1/T$ obtained at several heating rates yields a straight line, and the activation energy E can be determined from the slope.

Starink method

In this method, the approximation of $P(u)$ can be written as [31–33]:

$$P(u) \cong \frac{\exp(-1.0008u - 0.312)}{u^{1.92}} \tag{8}$$

Equations (4) and (8) lead to:

$$\ln\frac{\beta}{T^{1.92}} = -1.0008\frac{E}{RT} + C_2 \tag{9}$$

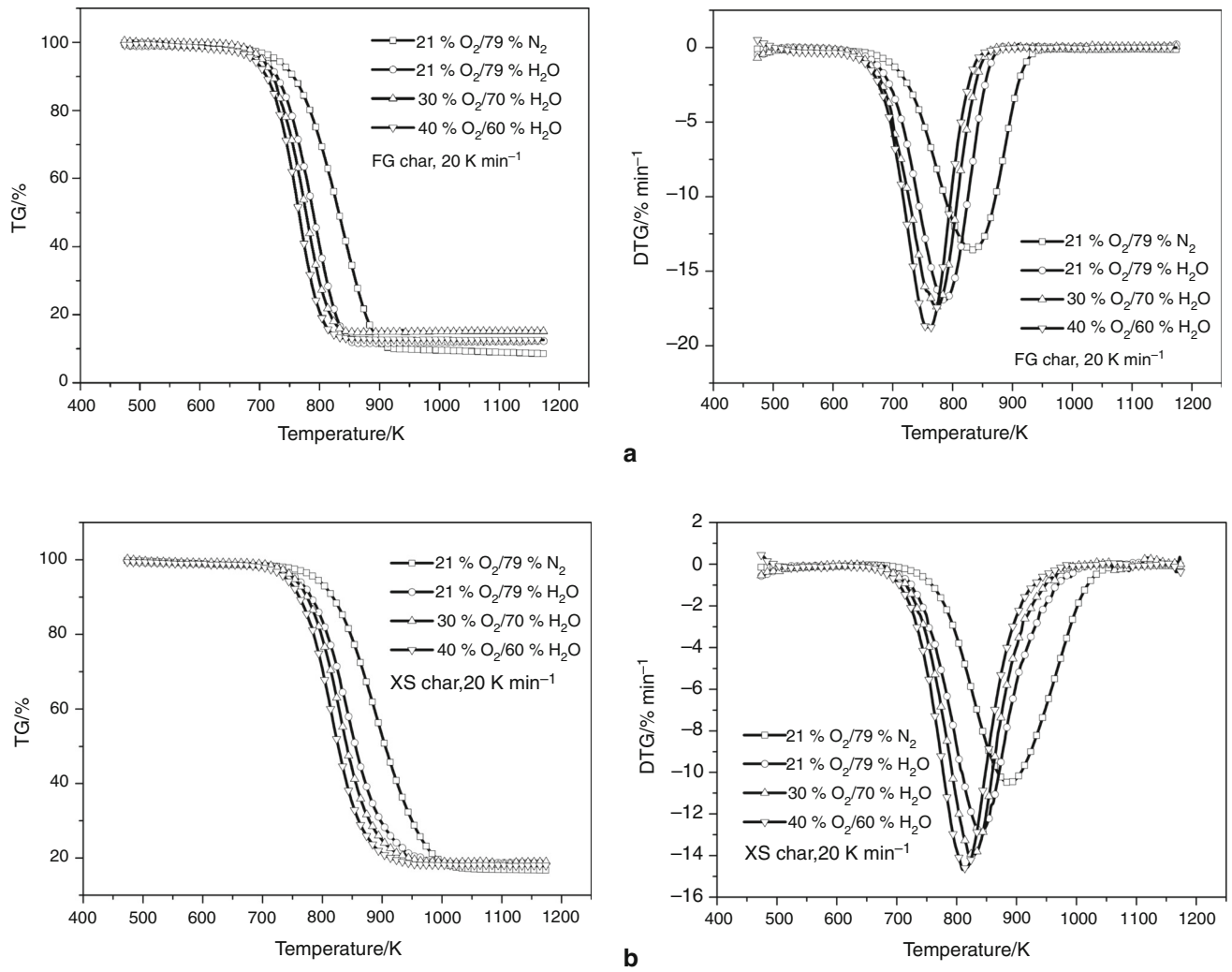

Fig. 1 TG and DTG curves of FG char (**a**) and XS char (**b**) combustion under different atmospheres

The activation energy E is determined from the slope of plots of $\ln(\beta/T^{1.92})$ versus $1/T$.

Kissinger–Akahira–Sunose (KAS) method

The expression of $P(u)$ is expressed using Murray and White approximation [34]:

$$P(u) \cong \frac{\exp(-u)}{u^2} \tag{10}$$

Based on this approximation, we obtain KAS equation:

$$\ln \frac{\beta}{T^2} = -\frac{E}{RT} + C_3 \tag{11}$$

For the same conversion ratio at different heating rates from plots of $\ln(\beta/T^2)$ versus $1/T$, the activation energy E can be determined by the slope.

Determination of the kinetic mechanism function

Popescu method The Popescu method [35] is used to determine the kinetic mechanism function of char combustion. This method can be expressed as:

$$G(a)_{\mathrm{mn}} = \int_{\alpha_{\mathrm{m}}}^{\alpha_{\mathrm{n}}} \frac{\mathrm{d}\alpha}{f(\alpha)} = \frac{1}{\beta}\int_{T_{\mathrm{m}}}^{T_{\mathrm{n}}} k(T)\mathrm{d}T = \frac{1}{\beta} I(T)_{\mathrm{mn}} = \frac{A}{\beta} H(T)_{\mathrm{mn}} \tag{12}$$

$$I(T)_{\mathrm{mn}} = \int_{T_{\mathrm{m}}}^{T_{\mathrm{n}}} k(T)\mathrm{d}T \tag{13}$$

$$H(T)_{\mathrm{mn}} = (T_{\mathrm{n}} - T_{\mathrm{m}}) \exp\left(-\frac{E}{RT_{\xi}}\right) \tag{14}$$

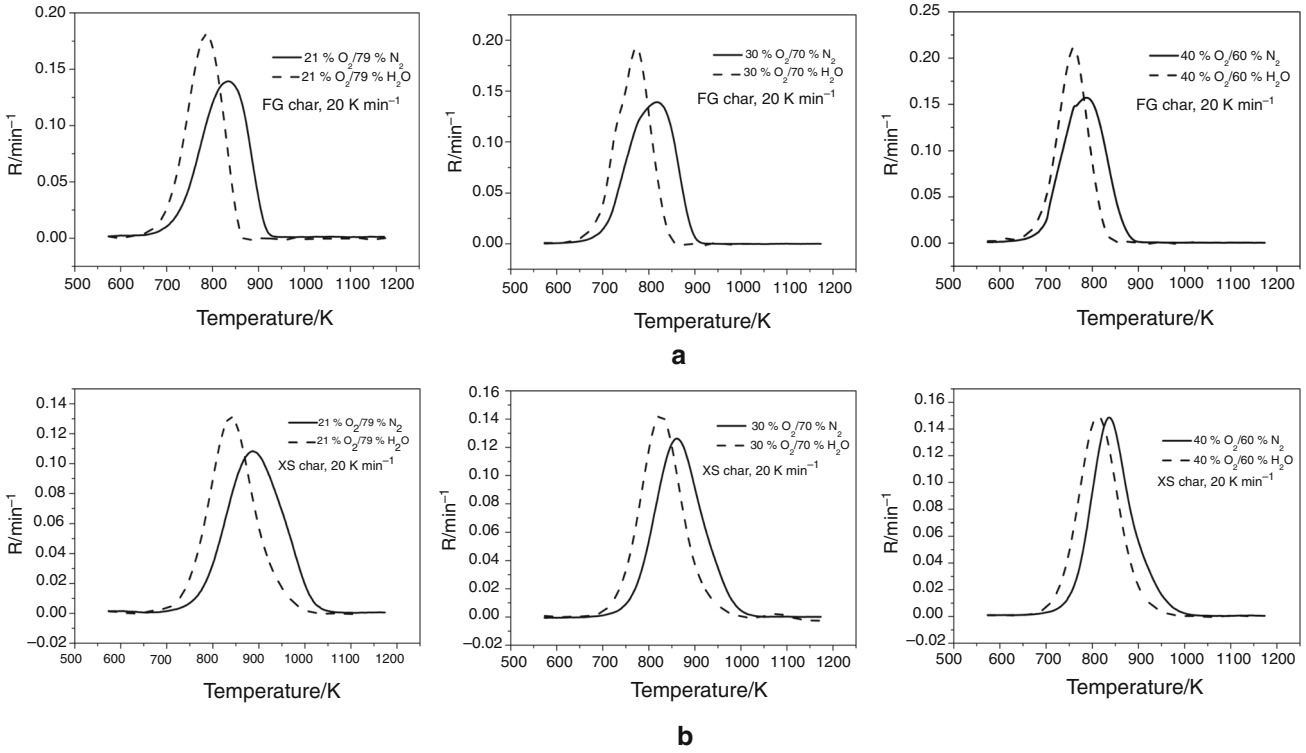

Fig. 2 Comparison of FG char (**a**) and XS char (**b**) reactivity versus temperature under different atmospheres

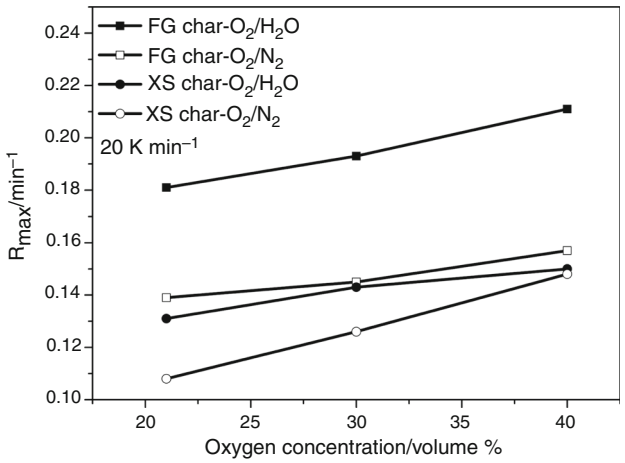

Fig. 3 Comparison of FG and XS char peak reactivity under different atmospheres

$$T_{\xi} = \frac{T_{\mathrm{m}} + T_{\mathrm{n}}}{2} \tag{15}$$

where X_{m} and X_{n} are two different degrees of the conversion ratio at temperatures T_{m} and T_{n}, respectively. If the experimental data and $G(a)$ are selected properly, a plot of $G(a)$ versus $1/\beta$ yields a straight line with an intercept of zero. This $G(a)$ is then a proper mechanism that describes the true chemical reaction process.

Coats–Redfern integral method

According to Eq. (4), the Coats–Redfern integral method can be written as:

$$\ln\left[\frac{G(a)}{T^2}\right] = \ln\left[\frac{AR}{\beta E}\left(1 - \frac{2RT}{E}\right)\right] - \frac{E}{RT} \tag{16}$$

At certain temperatures, the plots of $\ln [G(a)/T^2]$ versus $1/T$ obtained from the thermogravimetric data should be a straight line, and the activation energy E can be determined by the slope of the line.

Results and discussion

Combustion characteristics of coal char in O_2/H_2O atmosphere

Figure 1 shows the TG and DTG curves of FG and XS char combustion under different atmospheres. From the combustion profiles, it can be found that the char combustion process in the O_2/H_2O atmosphere is obviously different from that in O_2/N_2 atmosphere with the identical oxygen concentration. Replacing N_2 by H_2O has a significant influence on the char combustion under the conditions of the experiments. The combustion process of FG and XS char in O_2/H_2O atmosphere takes place sooner than that in

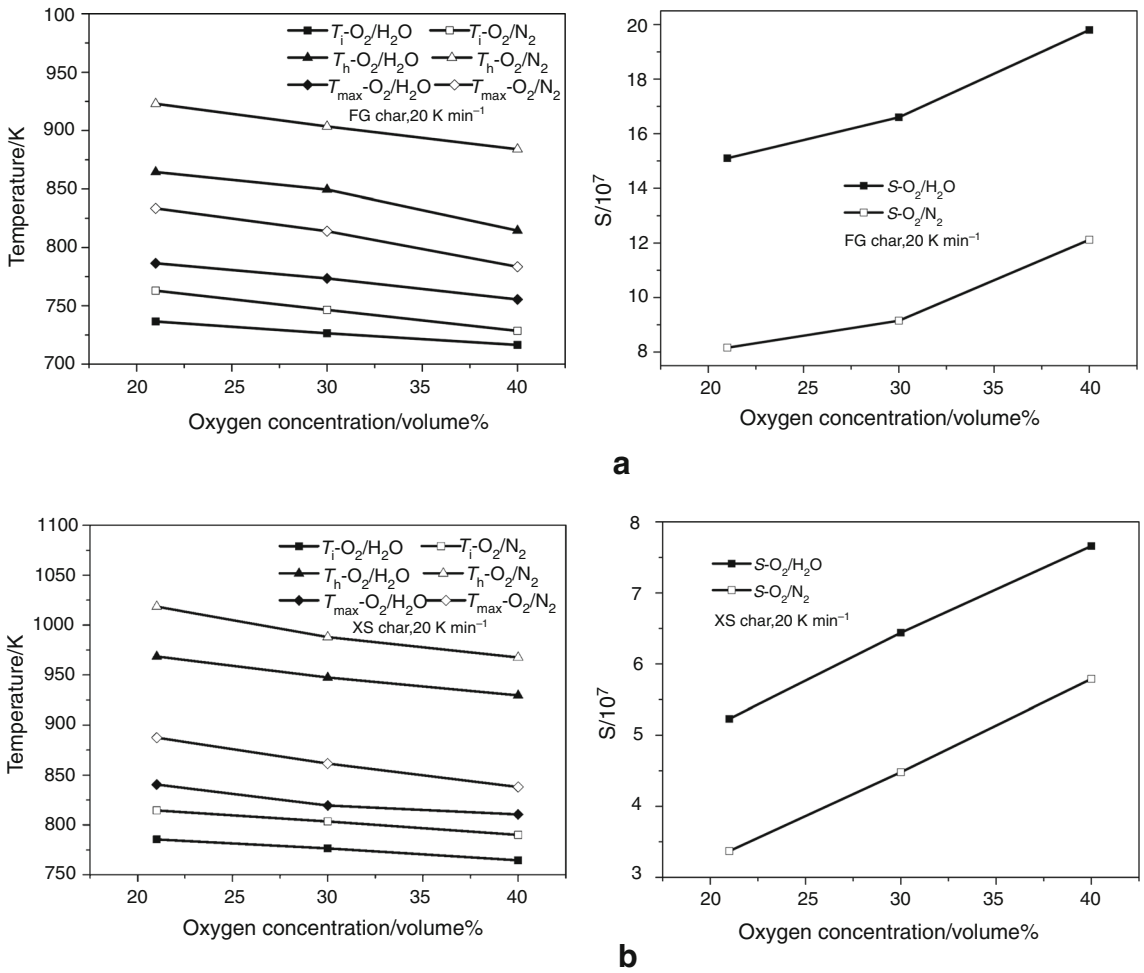

Fig. 4 Combustion characteristic temperatures and the comprehensive combustibility index S of FG char (**a**) and XS char (**b**) under different atmospheres

O_2/N_2 atmosphere with the identical oxygen concentration, and the combustion performance is improved by increasing oxygen concentration. The DTG curves shift to lower-temperature zone along with oxygen concentration increasing.

Figures 2 and 3 show the comparison of char reactivity R and peak reactivity R_{max} of FG and XS char under different atmospheres. Figure 2 indicates the substitution of H_2O for N_2 in the bulk gas has apparent effect on the char reactivity. The char reactivity in O_2/H_2O atmosphere is higher than that in O_2/N_2 atmosphere with the identical oxygen concentration for both FG and XS char. Figure 3 also shows the R_{max} of FG char is higher than that of XS char. The effect of oxygen concentration on the char reactivity in both atmospheres is also clear. The char reactivity increases with increasing oxygen concentration in both O_2/H_2O and O_2/N_2 mixtures, and it is found to be proportional to the oxygen concentration.

Figure 4 shows the combustion characteristic temperatures and the comprehensive combustibility index S of FG and XS char in different atmospheres with various oxygen concentrations (21, 30, 40 %). Figure 4 shows that the ignition temperature, peak temperature and burnout temperature in O_2/H_2O atmosphere are lower than those in O_2/N_2 atmosphere with the identical oxygen concentration, which indicates the combustion rate of char in O_2/H_2O atmosphere is faster compared with that in O_2/N_2 atmosphere. Figure 4 also shows that the comprehensive combustibility indexes in O_2/H_2O atmosphere are higher than those in O_2/N_2 atmosphere under the same oxygen concentration. The combustion performance of FG and XS char is improved when the diluent gas is changed from N_2 to H_2O.

The higher char reactivity and combustibility index in O_2/H_2O atmosphere may be due to the high reactivity and diffusivity of steam. The mole fractions of some active radicals, such as O and OH, in O_2/H_2O atmosphere are larger than those in O_2/N_2 atmosphere with the identical O_2 concentration due to high reactivity of H_2O [36]. These active radicals can be conducive to the oxidation of char. In

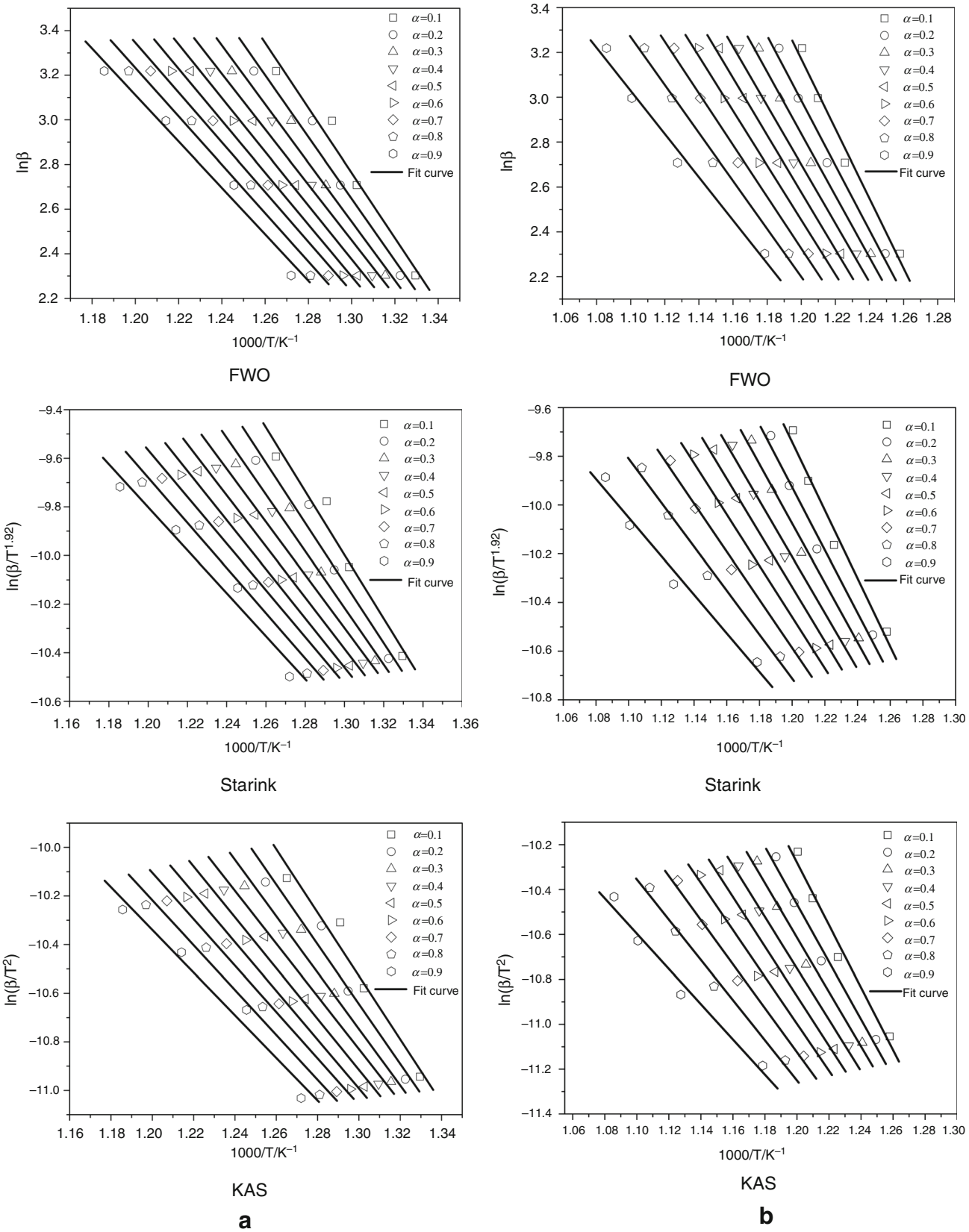

Fig. 5 Arrhenius plots proposed by different models at various conversion degrees of FG char (**a**) and XS char (**b**)

Table 2 Kinetic parameters and correlation coefficients of FG char calculated by different methods

Conversion/methods	FWO		Starink		KAS	
α	E/kJ mol^{-1}	R^2	E/kJ mol^{-1}	R^2	E/kJ mol^{-1}	R^2
0.1	127.56	0.985	109.04	0.981	108.44	0.981
0.2	121.17	0.985	102.87	0.982	102.27	0.981
0.3	115.18	0.988	97.09	0.984	96.49	0.984
0.4	108.71	0.988	90.86	0.985	90.26	0.985
0.5	105.36	0.989	87.59	0.986	86.99	0.985
0.6	101.81	0.991	84.14	0.987	83.54	0.987
0.7	97.58	0.99	80.02	0.987	79.43	0.986
0.8	94.89	0.989	77.38	0.985	76.78	0.985
0.9	91.04	0.988	73.61	0.983	73	0.983

Table 3 Kinetic parameters and correlation coefficients of XS char calculated by different methods

Conversion/methods	FWO		Starink		KAS	
α	E/kJ mol^{-1}	R^2	E/kJ mol^{-1}	R^2	E/kJ mol^{-1}	R^2
0.1	136.03	0.991	116.42	0.988	115.79	0.988
0.2	126.46	0.993	107.21	0.991	106.57	0.991
0.3	120.53	0.995	101.45	0.993	100.82	0.993
0.4	114.79	0.995	95.88	0.993	95.25	0.993
0.5	111.43	0.996	92.56	0.995	91.93	0.995
0.6	106.32	0.996	87.59	0.995	86.95	0.995
0.7	100.82	0.996	82.21	0.994	81.58	0.994
0.8	93.53	0.996	75.11	0.994	74.47	0.994
0.9	84.11	0.992	65.91	0.988	65.27	0.988

Table 4 BET surface area and average pore size of FG and XS char

Sample	BET surface area/m^2 g^{-1}	Average pore size/nm
FG char	25.13	7.38
XS char	12.61	15.01

addition, as the char combustion reaction progresses, the influence of diffusion on the char combustion becomes more pronounced [37]. The diffusion coefficient of O_2 in H_2O is 8.6E−5 m^2 s^{-1} (773 K, 0.1 MPa) and almost 25 % higher than that of O_2 in N_2 (6.4E−5 m^2 s^{-1}, 773 K, 0.1 MPa). Consequently, the probability of collision of O_2 to the surface of char in O_2/H_2O atmosphere is much higher than that in O_2/N_2 atmosphere, and it also contributes to the acceleration of the char combustion rate.

Activation energy of char combustion in 21 % O_2/79 % H_2O atmosphere

Activation energy is the most important kinetic parameter of char combustion and can be calculated from the experimental data of non-isothermal thermogravimetric tests. Model-fitting and model-free methods are two commonly used methods to calculate the activation energy. The advantages and limitations of the two methods have been discussed in numerous reports [29, 38]. Model-free methods are regarded as the most reliable methods for the determination of activation energy. Hence, three model-free methods are used in this study to determine the activation energies of char combustion.

In the model-free methods, a set of conversion values at different heating rates should be chosen from the thermogravimetric experimental data to determine the activation energy. Because most solid-state reactions are not stable at the beginning and the end of the reaction, which result in the deviation of experimental values from the theoretical data [39, 40], the range of conversion from 0.1 to 0.9 is chosen in our study.

According to Eqs. (7), (9) and (11), the plots of (1) ln β versus 1/T; (2) ln($\beta/T^{1.92}$) versus 1/T; (3) ln(β/T^2) versus 1/T at each chosen α and the corresponding linear fitting by the least-squares method are shown in Fig. 5. The kinetic

Table 5 Correlation coefficients (R^2) and standard deviations (SD) of the possible reaction models determined by the Popescu method

No.	Model	Symbol	Reaction mechanism	G/α	FG char	
					R^2	SD
2	Diffuse	D2	Two-dimensional, Valensi equation	$\alpha + (1-\alpha)\ln(1-\alpha)$	0.998	0.014
4	Diffuse	2D	Two-dimensional, Jander equation, $n = 2$	$[1-(1-\alpha)^{1/2}]^2$	0.998	0.009
6	Diffuse	D3	Three-dimensional, Jander equation	$[1-(1-\alpha)^{1/3}]^2$	0.996	0.008
7	Diffuse	D4	Three-dimensional, Ginstring–Brounshtein equation	$1-\frac{2}{3}\alpha-(1-\alpha)^{2/3}$	0.999	0.003
16	Chemical reaction	F1	First-order reaction	$-\ln(1-\alpha)$	0.996	0.012

Table 6 Results from the application of the Coats–Redfern integral method for the possible kinetic models

No.	E/kJ mol^{-1}	A/s^{-1}	R^2	SD
2	196.72	1.9E+18	0.972	0.328
4	210.52	2.6E+19	0.978	0.307
6	223.86	2.7E+20	0.983	0.288
7	205.65	3.6E+18	0.976	0.315
16	122.08	4.4E+11	0.989	0.123

parameters and the correlation coefficients of linear fitting for each method are listed in Tables 2 and 3.

Tables 2 and 3 show that the correlation coefficients are all higher than 0.98, which indicates that the linear correlation is quite good. In Tables 2 and 3, the activation energies calculated from FWO, Starink and KAS decrease with the increase in the conversion level. The reasons for this behavior may be associated with the combustion control mechanism [37, 41]. The char combustion is under kinetic control at low temperatures (low conversion level). As the reaction proceeds, the reaction rate of the char increases, and the amount of ash accumulating at the particle surfaces increases, resulting in the inhibition of O_2 diffusion to the surface of the char particle. Consequently, the control mechanism is changed from kinetic control at low temperatures to the combined control of the kinetics and diffusion at high temperatures. Moreover, the catalysis of minerals and the change in the pore structure may result in the increase in the char reactivity [42–45]. Liu [37] and Wang et al. [46] also reached similar conclusions in their experiments on char combustion in oxy-fuel atmospheres.

In Tables 2 and 3, at a given conversion ratio, the activation energy of FG char is less than that of XS char. This difference may be attributed to the different compositions of char sample and the evolution of the pore structure during devolatilization. The char reactivity decreases with increasing ash content due to the presence of ash on the surface [45]. As given in Table 1, the ash content of the FG char sample is lower than that of the XS char sample, resulting in the lower activation energy of the FG char sample compared with the XS char sample. Table 4 shows the pore parameters of the FG and XS char samples. The Brunauer–Emmett–Teller (BET) surface area of FG char (25.13 m^2 g^{-1}) is higher than that of XS char (12.61 m^2 g^{-1}). Because the higher specific surface area of the char results in a higher reactivity [47], the combustion reactivity of FG char is higher than that of XS char.

Kinetic mechanism function of char combustion in 21 % O_2/79 % H_2O atmosphere

According to the Popescu method, 41 typical mechanisms are analyzed [48]. The calculated values of correlation coefficients R^2 and standard deviations SD are used as criteria for all candidate reaction models ($R^2 > 0.996$ and SD < 0.02). The seven reaction mechanism models meeting the criteria are listed in Table 5 for FG char. Based on the mechanism functions listed in Table 5, the Coats–Redfern integral method is used to determine the active activation energy.

Table 6 shows the kinetic parameters of FG char obtained by the Coats–Redfern integral method at 25 K min^{-1}. The kinetic parameters are found to strongly depend on the reaction model. According to R^2 and SD, the No. 16 chemical reaction (first-order) model is the most suitable for FG char and the corresponding activation energy is 122.08 kJ mol^{-1}. The activation energy of FG char is in the range of activation energy values (91.04–127.56 kJ mol^{-1}) obtained by the FWO method. Consequently, the combustion mechanism function of FG char in O_2/H_2O is $-\ln(1-a)$. This result demonstrates that the combustion of FG char in O_2/H_2O atmosphere follows the first-order chemical reaction kinetic.

Conclusions

The combustion and kinetic behaviors of two coal char samples (FG and XS) in O_2/H_2O atmosphere were investigated using non-isothermal thermogravimetric analysis. According to the TG–DTG curves, replacing N_2 by H_2O

had a significant influence on the char combustion under the conditions of the experiment. The combustion reactivity and performance of FG and XS char were improved in O_2/H_2O atmosphere compared with O_2/N_2 atmosphere with the identical oxygen concentration due to the high reactivity and diffusivity of H_2O. Meanwhile, the ignition temperature, peak temperature and burnout temperature in O_2/H_2O atmosphere were lower than those in O_2/N_2 atmosphere with the identical oxygen concentration. The activation energies of FG and XS char obtained by the FWO, Starink and KAS methods decreased with the increasing conversion level because of the change in the combustion control mechanism, and the activation energy of FG char was less than that of XS char. The combustion of FG char in O_2/H_2O atmosphere was found to follow the first-order chemical reaction kinetic.

Acknowledgements This work was supported by the general program (51176055) of the National Natural Science Foundation of China and the National Key Basic Research and Development Program of China (Grant No. 2011CB707301). The authors gratefully thank the State Key Laboratory of Engines of Tianjin University.

References

1. IPCC. Summary for policymakers. In: Solomon S, Qin D, Manning M, Chen Z, Marquis M, Averyt KB, Tignor M, Miller HL, editors. Climate change 2007: the physical science basis. Contribution of working group I to the fourth assessment report of the intergovernmental panel on climate change. Cambridge: Cambridge University Press; 2007. p. 2–4.
2. Edge P, Gharebaghi M, Irons R, Porter R, Porter RTJ, Pourkashanian M, Smithc D, Stephensond P, Williamsa A. Combustion modelling opportunities and challenges for oxy-coal carbon capture technology. Chem Eng Res Des. 2011;89:1470–93.
3. Chen L, Yong SZ, Ghoniem AF. Oxy-fuel combustion of pulverized coal: characterization, fundamentals, stabilization and CFD modeling. Prog Energy Combust Sci. 2012;38:156–214.
4. Toftegaard MB, Brix J, Jensen PA, Glarborg P, Jensen AD. Oxy-fuel combustion of solid fuels. Prog Energy Combust Sci. 2010;36:581–625.
5. Salvador C, Mitrovic M, Kourash K. Novel oxy-steam burner for zero-emission power plants. 2009. http://www.ieaghg.org/docs/oxyfuel/OCC1/Session%206_C/2_NOVEL%20OXY-STEAM%20BURNER%20FOR%20ZERO-EMISSION%20POWER%20PLANTS.pdf.
6. Salvador C. Modeling design and pilot-scale experiments of CANMET'S advanced oxy-fuel/steam burner. In: International oxy-combustion reserch network 2nd workshop. USA; 25, 26 Jan 2007.
7. Seepana S, Jayanti S. Steam-moderated oxy-fuel combustion. Energy Convers Manage. 2010;51:1981–8.
8. Rathnam RK, Elliott LK, Wall TF, Liu Y, Moghtaderi B. Differences in reactivity of pulverised coal in air (O_2/N_2) and oxy-fuel (O_2/CO_2) conditions. Fuel Process Technol. 2009;90(6):797–802.
9. Buhre B, Elliott L, Sheng C, Gupta R, Wall T. Oxy-fuel combustion technology for coal-fired power generation. Prog Energy Combust Sci. 2005;31(4):283–307.
10. Kuehl D. Effects of water on burning velocity of hydrogen-air flames. ARSJ-AM Rocket Soc J. 1962;32:1724–6.
11. Babkin V, V'yun A. Effect of water vapor on the normal burning velocity of a methane-air mixture at high pressures. Combust Explo Shock+. 1971;7(3):339–41.
12. Koroll G, Mulpuru S. The effect of dilution with steam on the burning velocity and structure of premixed hydrogen flames. Symp Int Combust. 1988;21(1):1811–9.
13. Liu D, MacFarlane R. Laminar burning velocities of hydrogen-air and hydrogen-air steam flames. Combust Flame. 1983;49(1):59–71.
14. Boushaki T, Dhué Y, Selle L, Ferret B, Poinsot T. Effects of hydrogen and steam addition on laminar burning velocity of methane–air premixed flame: experimental and numerical analysis. Int J Hydrog Energy. 2012;37(11):9412–22.
15. Mazas A, Fiorina B, Lacoste D, Schuller T. Effects of water vapor addition on the laminar burning velocity of oxygen-enriched methane flames. Combust Flame. 2011;158(12):2428–40.
16. Gil M, Riaza J, Álvarez L, Pevida C, Pis J, Rubiera F. A study of oxy-coal combustion with steam addition and biomass blending by thermogravimetric analysis. J Therm Anal Calorim. 2011;109(1):49–55.
17. Yi B, Zhang L, Huang F, Mao Z, Zheng C. Effect of H_2O on the combustion characteristics of pulverized coal in O_2/CO_2 atmosphere. Appl Energy. 2014;132:349–57.
18. Riaza J, Álvarez L, Gil M, Pevida C, Pis J, Rubiera F. Effect of oxy-fuel combustion with steam addition on coal ignition and burnout in an entrained flow reactor. Energy. 2011;36(8):5314–9.
19. Hecht ES, Shaddix CR, Geier M, Molina A, Haynes BS. Effect of CO_2 and steam gasification reactions on the oxy-combustion of pulverized coal char. Combust Flame. 2012;159(11):3437–47.
20. Zou C, Zhang L, Cao S, Zheng C. A study of combustion characteristics of pulverized coal in O_2/H_2O atmosphere. Fuel. 2014;115:312–20.
21. Zou C, Cai L, Wu D, Liu Y, Liu S, Zheng C. Ignition behaviors of pulverized coal particles in O_2/N_2 and O_2/H_2O mixtures in a drop tube furnace using flame monitoring techniques. Proc Combust Inst. 2015;35(3):3629–36.
22. Cai L, Zou C, Liu Y, Zhou K, Han Q, Zheng C. Numerical and experimental studies on the ignition of pulverized coal in O_2/H_2O atmospheres. Fuel. 2015;139:198–205.
23. Li Q, Zhao C, Chen X, Wu W, Li Y. Comparison of pulverized coal combustion in air and in O_2/CO_2 mixtures by thermogravimetric analysis. J Anal Appl Pyrolysis. 2009;85:521–8.
24. Wang C, Zhang X, Liu Y, Che D. Pyrolysis and combustion characteristics of coals in oxyfuel combustion. Appl Energy. 2012;97:264–73.
25. Xu Y, Zhang Y, Zhang G, Guo Y, Zhang J, Li G. Pyrolysis characteristics and kinetics of two Chinese low-rank coals. J Therm Anal Calorim. 2015;122(2):975–84.
26. Zhang Y, Zhang L, Duan F, Jiang X, Sun X, Chyang C. Co-combustion characteristics of sewage sludge with different rank bituminous coals under the O_2/CO_2 atmosphere. J Therm Anal Calorim. 2015;121(2):729–36.
27. Deng J, Wang K, Zhang Y, Yang H. Study on the kinetics and reactivity at the ignition temperature of Jurassic coal in North Shaanxi. J Therm Anal Calorim. 2014;118(1):417–23.
28. Flynn JH, Wall LA. A quick, direct method for the determination of activation energy from thermogravimetric data. J Polym Sci Part C Polym Lett. 1966;4:323–8.
29. Ozawa T. A new method of analyzing thermogravimetric data. Bull Chem Soc Jpn. 1965;38:1881–6.
30. Doyle CD. Estimating isothermal life from thermogravimetric data. J Appl Polym Sci. 1962;6:639–42.
31. Starink MJ. A new method for the derivation of activation energies from experiments performed at constant heating rate. Thermochim Acta. 1996;288:97–104.

32. Starink MJ. The determination of activation energy from linear heating rate experiments: a comparison of the accuracy of isoconversion methods. Thermochim Acta. 2003;404:163–76.
33. Starink MJ. Activation energy determination for linear heating experiments: deviations due to neglecting the low temperature end of the temperature integral. J Mater Sci. 2007;42:483–9.
34. Kissinger HE. Reaction kinetics in differential thermal analysis. Anal Chem. 1957;29:1702–6.
35. Popescu C. Integral method to analyze the kinetics of heterogeneous reactions under non-isothermal conditions a variant on the Ozawa–Flynn–Wall method. Thermochim Acta. 1996;285:309–23.
36. Zou C, Song Y, Li G, Cao S, He Y, Zheng C. The chemical mechanism of steam's effect on the temperature in methane oxy-steam combustion. Int J Heat Mass Transf. 2014;75:12–8.
37. Liu H. Combustion of coal chars in O_2/CO_2 and O_2/N_2 mixtures: a comparative study with non-isothermal thermogravimetric analyzer (TGA) tests. Energy Fuels. 2009;23:4278–85.
38. Vyazovkin S, Wight CA. Model-free and model-fitting approaches to kinetic analysis of isothermal and nonisothermal data. Thermochim Acta. 1999;340–341:53–68.
39. Janković B, Mentus S, Jelić D. A kinetic study of non-isothermal decomposition process of anhydrous nickel nitrate under air atmosphere. Phys B. 2009;404:2263–9.
40. Galwey AK. Solid state decompositions: the interpretation of kinetic and microscopic data and the formulation of a reaction mechanism. Thermochim Acta. 1985;96:259–73.
41. Liu X, Li B, Miura K. Analysis of pyrolysis and gasification reactions of hydrothermally and supercritically upgraded low-rank coal by using a new distributed activation energy model. Fuel Process Technol. 2001;69:1–12.
42. Lunden M, Yang N, Headley T, Shaddix C, Hardesty D. Mineral matter effects on char structural evolution and oxidation kinetics during coal char combustion. Sandia National Labs, Albuquerque; 1997.
43. Zhang H, Li H, Chen J, Zhao B, Hu G. The influence of included minerals on the intrinsic reactivity of chars prepared under N_2 and CO_2 environment. In: Qi H, Zhao B, editors. Cleaner combustion and sustainable world. London: Springer; 2013. p. 1219–23.
44. Chan ML, Jones JM, Pourkashanian M, Williams A. The oxidative reactivity of coal chars in relation to their structure. Fuel. 1999;78:1539–52.
45. Wang B, Sun L, Su S, Xiang J, Hu S, Fei H. Char structural evolution during pyrolysis and its influence on combustion reactivity in air and oxy-fuel conditions. Energy Fuels. 2012;26:1565–74.
46. Wang C, Liu Y, Zhang X, Che D. A study on coal properties and combustion characteristics of blended coals in northwestern china. Energy Fuels. 2011;25:3634–45.
47. Lee DW, Bae JS, Park SJ, Lee YJ, Hong JC, Choi YC. The pore structure variation of coal char during pyrolysis and its relationship with char combustion reactivity. Ind Eng Chem Res. 2012;51:13580–8.
48. Hu RZ, Shi QZ. Thermal analysis kinetics. Beijing: Science Press; 2001. p. 127–31 **(in Chinese)**.